

Supporting Information

Catalytic Reactivity of an Iridium Complex with a Proton Responsive N-Donor ligand in CO₂ Hydrogenation to Formate

Gunniya Hariyanandam Gunasekar,^{a†} Yeahsel Yoon,^{a†} Il-hyun Baek,^b and Sungho Yoon^{*a}

List of Figures

- Figure S1. Crystal structure of **1** in a unit cell
- Figure S2. Stabilization structure of **1**
- Figure S3. UV-Visible spectrum of **1**
- Figure S4. ESI-Mass spectrum of **1**.
- Figure S5. ¹H-NMR spectra of BiBzImH₂ ligand and **1**
- Figure S6. Expected structure of **1** under basic condition
- Figure S7. TOF between the hours
- Figure S8. ¹H-NMR spectrum of **1** after hydrogenation
- Figure S9. ESI-Mass spectrum of **1** after hydrogenation

List of Tables

- Table S1. Formate formation rate at each interval of time.
- Table S2. Comparison of bond lengths and angles of **1** with [Cp*Ir(Bpy)Cl]Cl
- Table S3. X-ray Crystallographic information of **1**

Figure S1. Crystal structure of **1** in a unit cell.

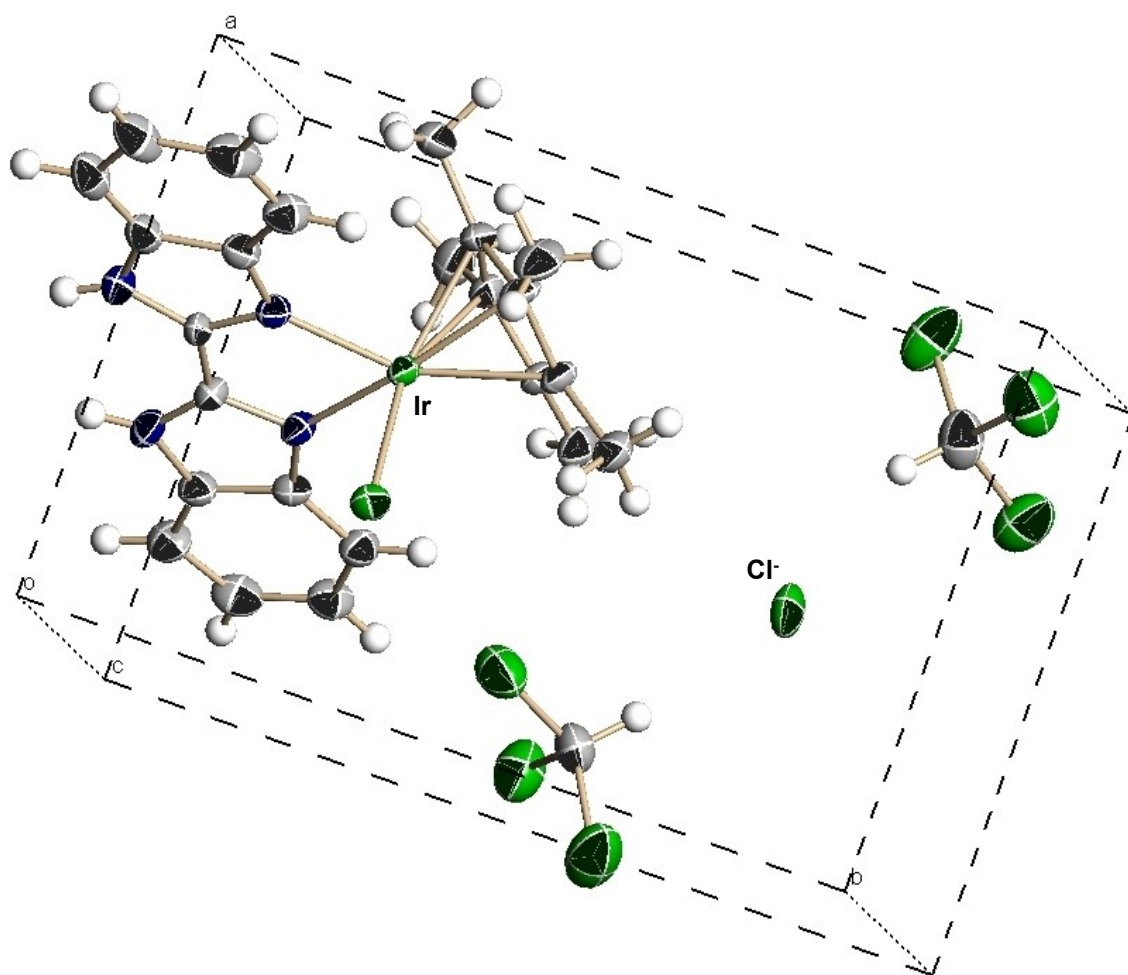
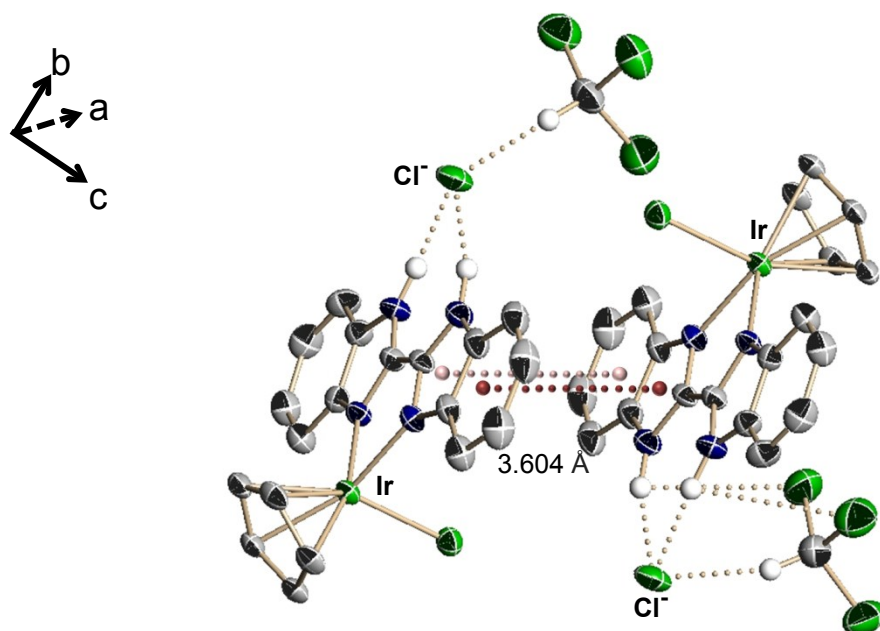


Figure S2. Stabilization structure of **1**. Protons on benzene ring and methyl groups on Cp* are omitted for clarity.



The crystal structure of **1** showed that the counter anion i.e. Cl⁻ formed a weak hydrogen bond with N-H unit of BiBzImH₂ and to C-H of chloroform. In addition, two molecules of **1** were stabilized through π - π interaction (of benzimidazole ring) with a distance of 3.604 Å.

Figure S3. UV-Visible spectrum of **1** in chloroform solution.

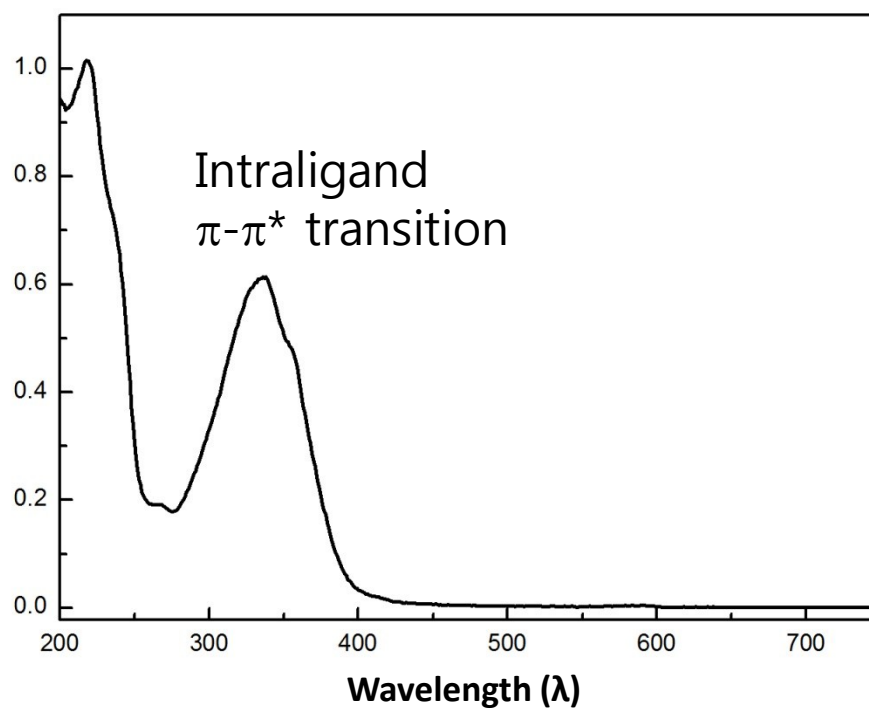


Figure S4. ESI-Mass spectra of **1**.

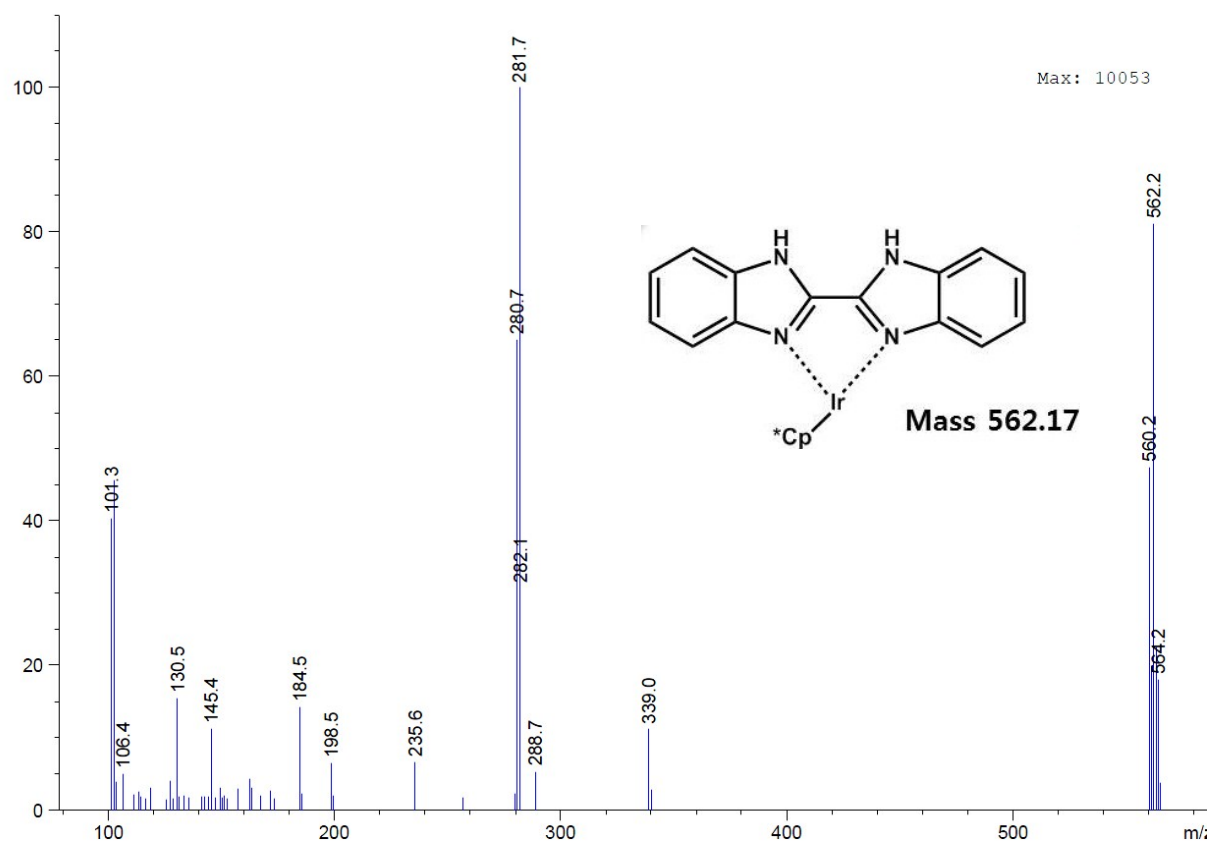


Figure S5. $^1\text{H-NMR}$ spectra of BiBzImH₂ ligand in DMSO-d₆ and **1** in CDCl₃

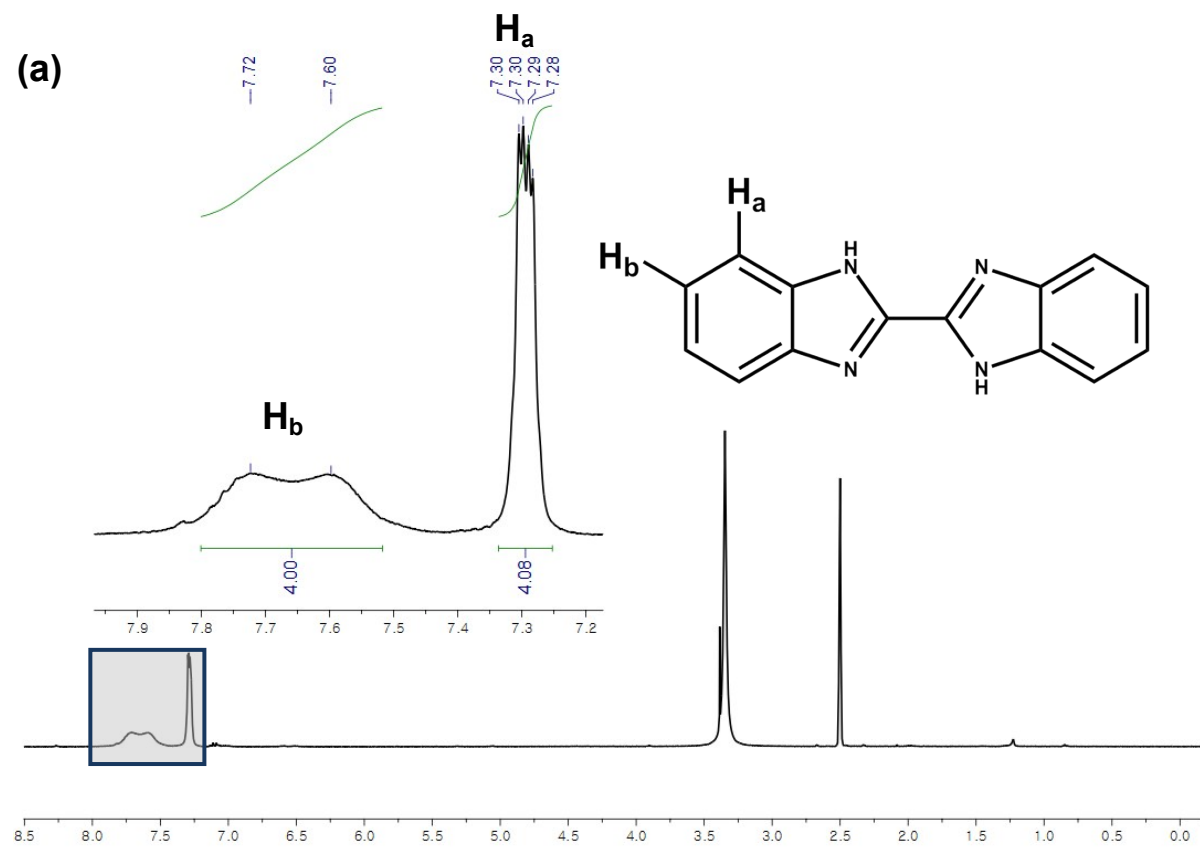
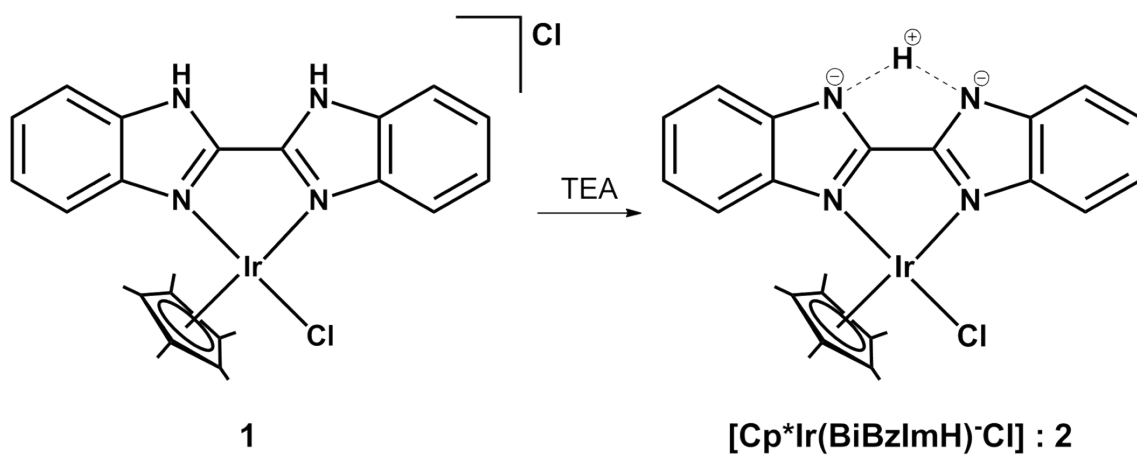
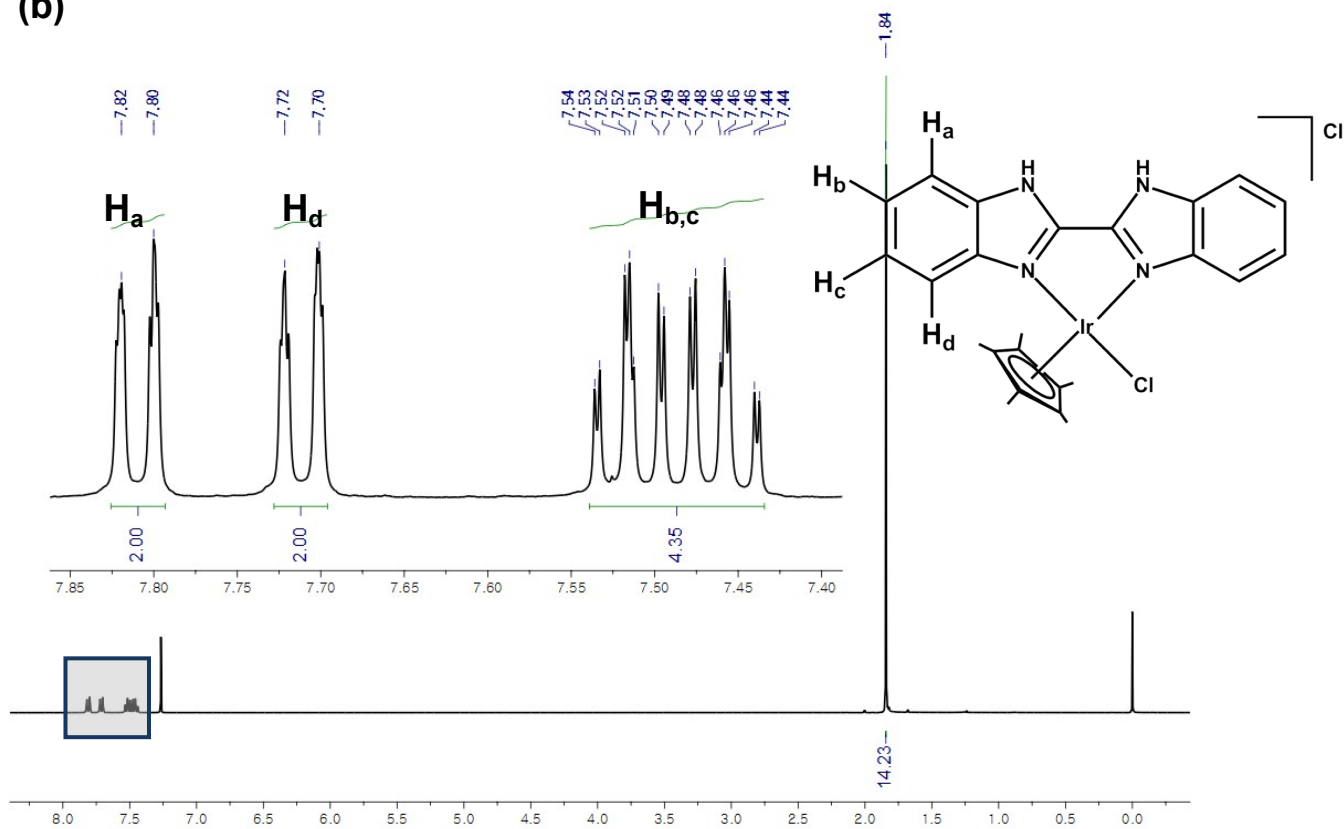


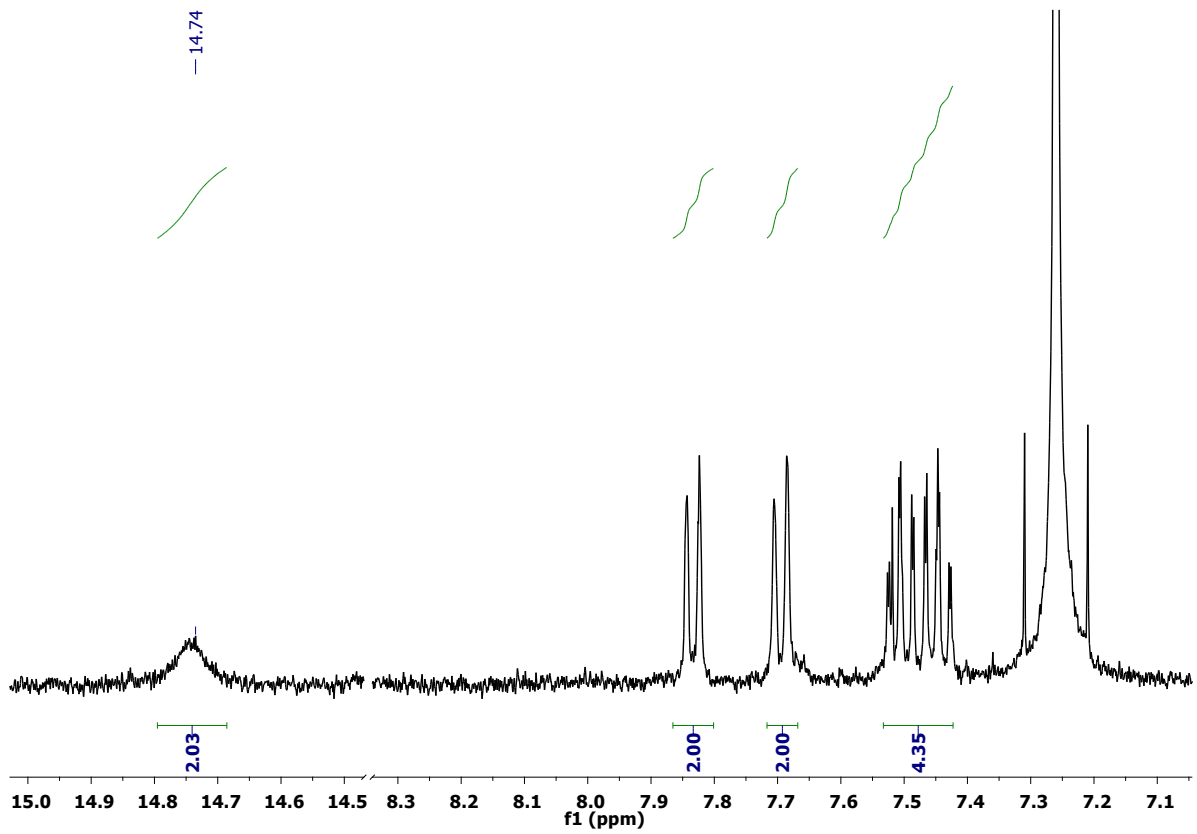
Figure S6. Expected structure of **1** under basic condition



(b)



(c)



(d)

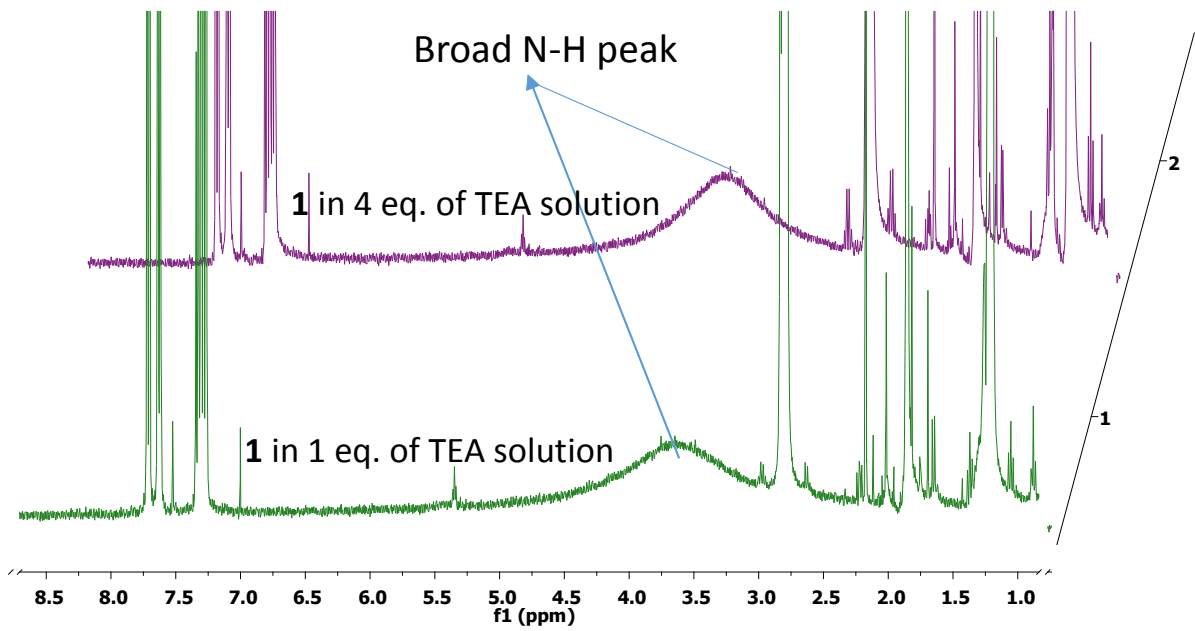


Figure S7. TOF between the time interval

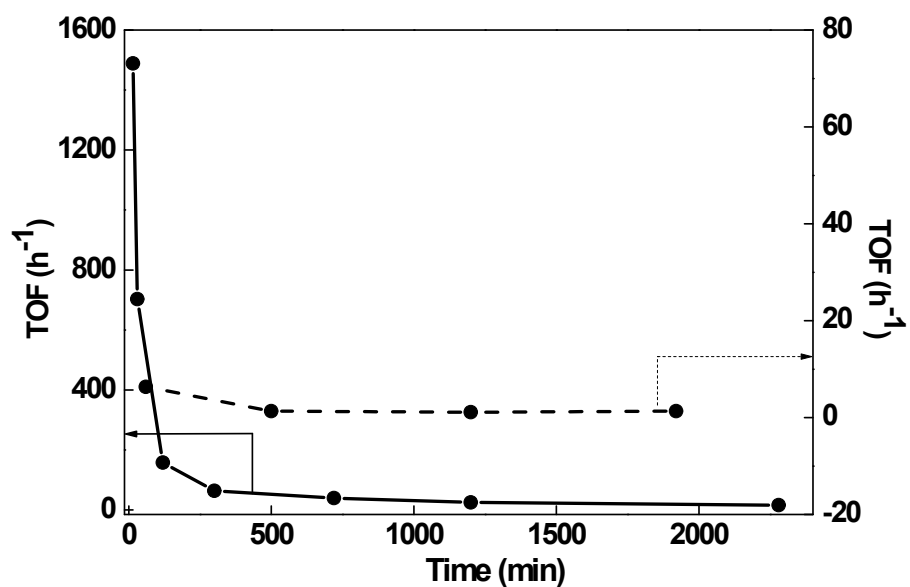


Figure S8. ¹H-NMR spectrum of 1 after hydrogenation

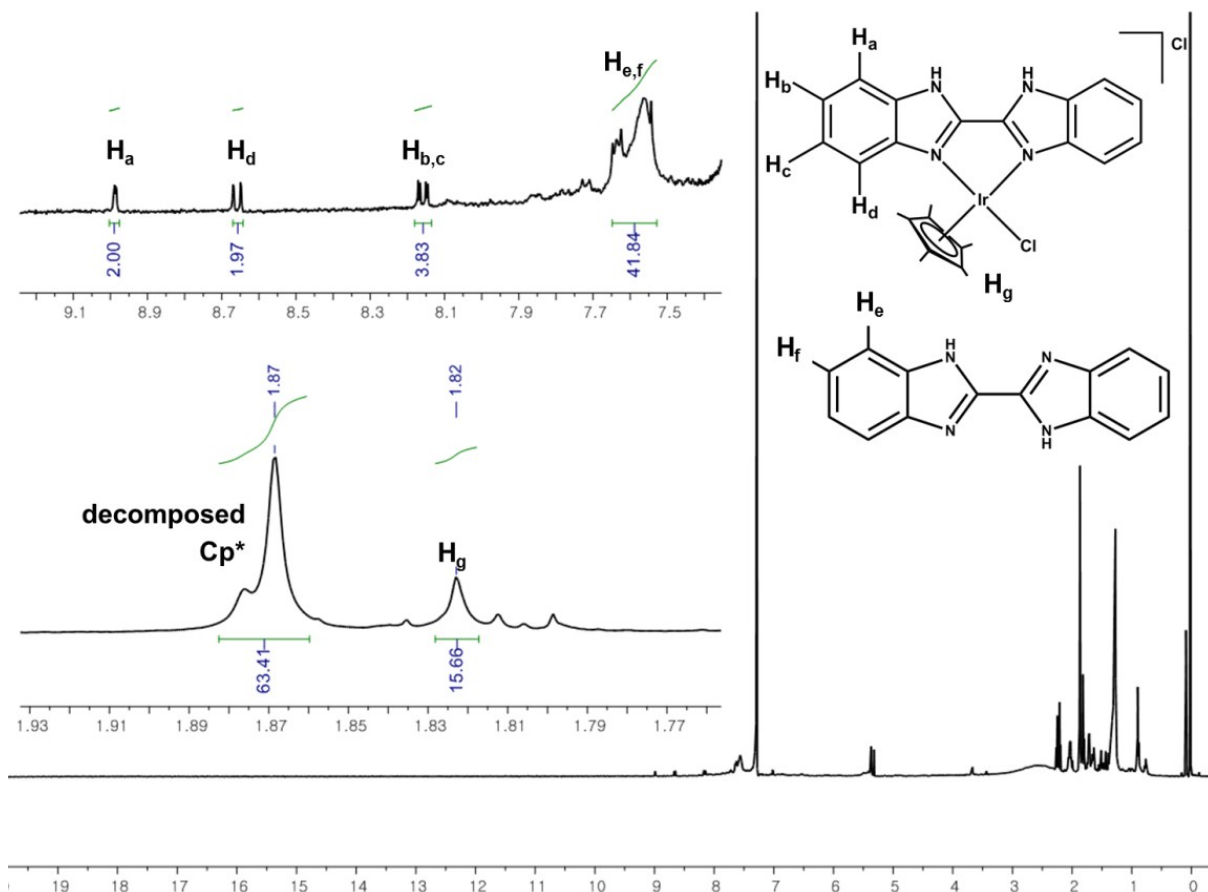


Figure S9. ESI-Mass spectrum of **1** after hydrogenation

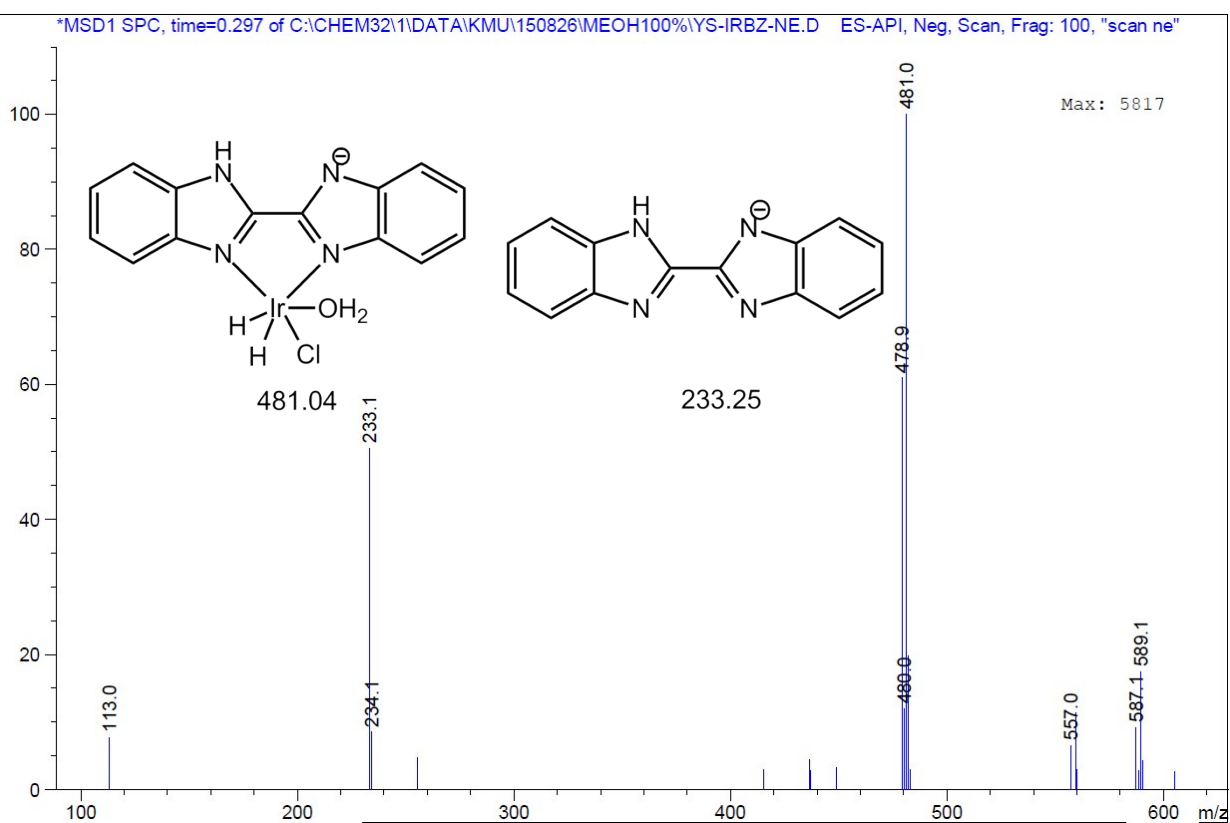
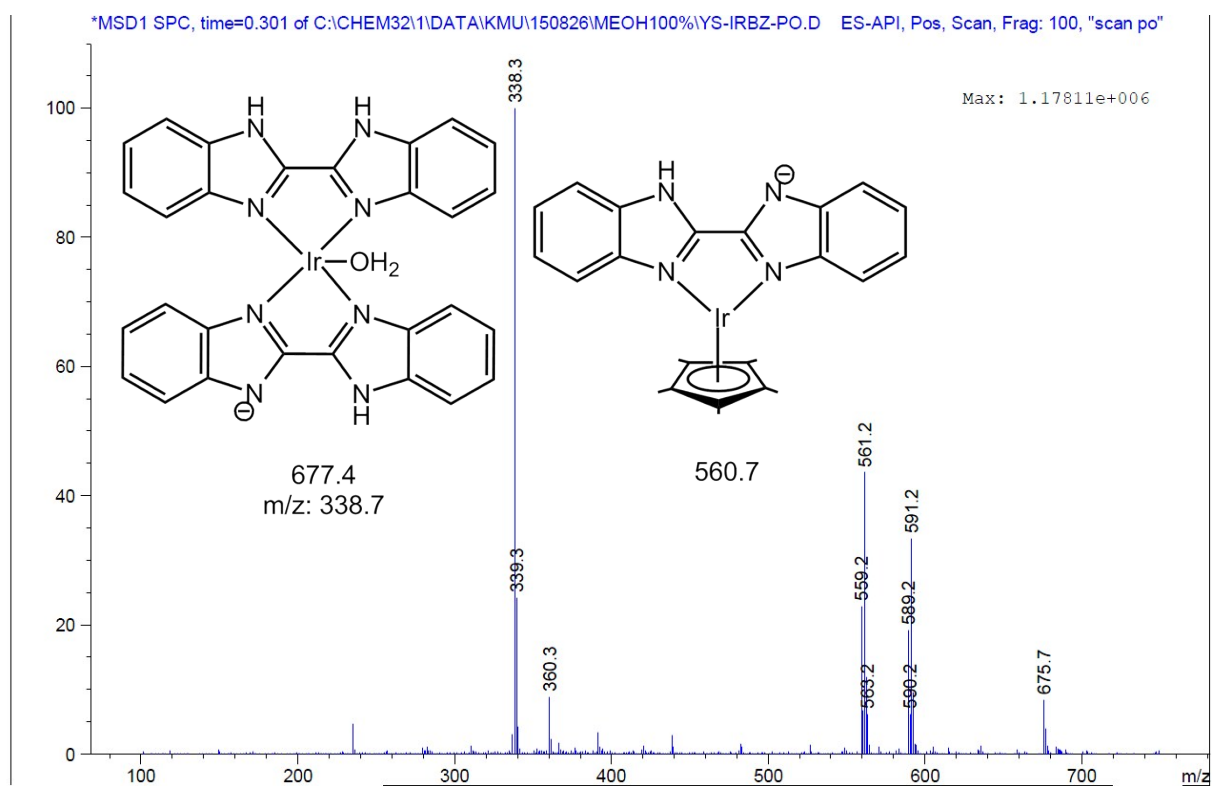


Table S1. TOF between the hours.

Time (min)	(TOF/h)
15	1500
30	700
120	158
300	65
720	40
1200	25
2280	16

Table S2. Comparison of bond lengths and angles of **1** with [Cp*Ir(Bpy)Cl]Cl

	[Cp*Ir(Bpy)Cl] ⁺	1
Ir-N (Å)	2.076 (8)	2.127(2)
	2.090 (9)	2.148(2)
Ir-Cl (Å)	2.404 (2)	2.3941(7)
Ir-Cp* Centroid(Å)*	1.785	1.789
N-Ir-Cl (°)	85.47	86.82
Distortion angle (°) (ligand-Ir)	3.38	6.32 (19)
Internal angle of N-C-C	112.94	114.55(18)

● **N-C-C Internal angle**

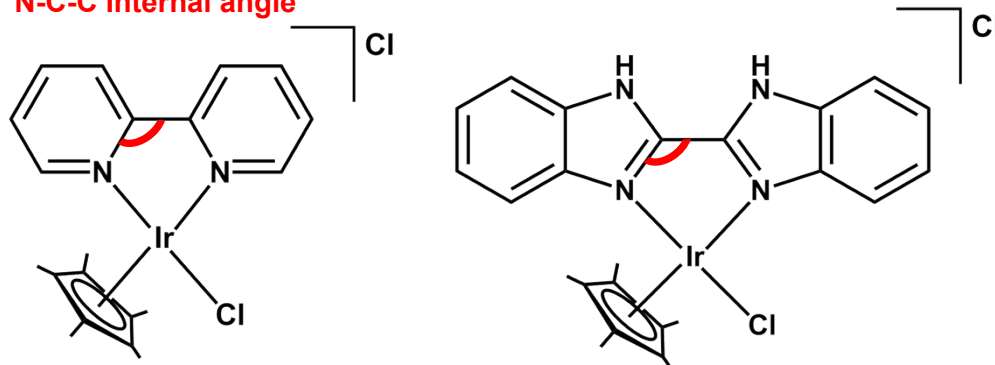


Table S3. X-ray Crystallographic information of **1**.

Formula	C ₂₆ H ₂₇ Cl ₈ IrN ₄
<i>M_r</i>	874.34
Crystal system	Monoclinic
Space group	<i>P2₁/n</i>
Crystal color and shape	Yellow block
Crystal size	0.09 x 0.16 x 0.20
<i>a</i> (Å)	8.3668(4)
<i>b</i> (Å)	12.3575(5)
<i>c</i> (Å)	30.7228(13)
<i>β</i> (°)	90.5240(10)
<i>V</i> (Å ³)	3176.4(2)
<i>Z</i>	4
<i>T</i> (K)	223(2)
<i>F</i> (000)	1708
Scan range (°)	2.52 < <i>θ</i> < 28.49
<i>R</i> _{int}	0.0269
Goodness-of-fit	0.925

$$R1 = \frac{\sum ||F_o| - |F_c||}{\sum |F_o|}; \quad wR2 = \left\{ \frac{\sum [w(|F_o|^2 - |F_c|^2)]^2}{\sum [w|F_o|^2]} \right\}^{1/2}$$